AN IMAGE ANALYSIS METHOD TO QUANTIFY FIBRE SEPARATION IN WOOD SUBJECTED TO FATIGUE LOADING

Ramesh Thiruvengadaswamy
Postdoctoral fellow
Dept. of Mechanical Engineering

Daniel Ouellet
Research Engineer, Pulp and Paper Research Institute of Canada
Adjunct Professor, Dept. of Mechanical Engineering

University of British Columbia
Pulp and Paper Centre
2385 East Mall, Vancouver, BC
Canada, V6T 1Z4

ABSTRACT

Fundamental aspects of mechanical pulping have often been studied by subjecting wood samples to cyclic loads under controlled laboratory conditions. Several methods have been developed to quantify fatigue damage in these samples, but none of them provides a direct measure of the degree of fibre separation resulting from the formation of cracks. This makes it difficult to understand the early stages of wood breakdown. To address this problem, we have developed an image analysis method to quantify the degree of fibre separation observed in transverse cross-sections of wood samples. The method was used to assess the effect of strain, strain rate, temperature and number of cycles on fibre separation in samples subjected to radial compression. The efficiency of various loading conditions was assessed by plotting the fibre separation index against specific energy consumption. The results indicate that strain rate strongly affects the efficiency of fibre separation. In general, a higher temperature (96^{o}C vs 25^{o}C) resulted in a lower proportion of separated fibres, but at a much lower energy requirement, thus leading to more efficient fibre separation. The image analysis method offers a reliable way to characterize fibre separation. The method also has the unique advantage of being applicable to samples loaded under any combination of compression and shear, which opens the door for a comparison of these modes of loading in future work.

INTRODUCTION

In mechanical pulping by refining, wood chips are disintegrated into pulp between opposing discs, one or both of which rotate. The discs are fitted with plates that have a pattern of bars and grooves. Under such conditions, the chips are subjected to repeated shear and compression at high temperatures and strain rates. This can produce fibre failure (in the form of lumen collapse, external and internal fibrillation), softening of wood components and separation of fibres.

Though it is believed that some kind of fatigue mechanism is involved in the process of fibre separation [1-5], relatively little is known about the actual mechanism.

Salmén *et al*. monitored changes in elastic modulus to compare the efficiency of defibration and observed a sharp reduction in modulus in the early stages of cycling [6,7]. The later stages of cycling produced much smaller changes in modulus. Further, similar reductions in modulus were achieved in fewer cycles at higher stress amplitudes. Uhmeier [8] extended a part of the study of Salmén *et al*. to higher strain levels to account for large loads and plastic strains. He found that a few large compressions were sufficient to increase the collapsibility of earlywood fibres.

In our previous work aimed at understanding fibre separation, we have examined changes in modulus to characterize fatigue damage in wood samples subjected to large cyclic strains [9-11]. Our results have shown that the evolution of modulus is not a reliable way to quantify fibre separation under such loading conditions.

Besides methods based on modulus, other techniques have also been used to understand the behaviour of wood in mechanical pulping. Berg monitored acoustic emission activity to investigate the effect of temperature, strain and loading direction on fracture history during compression of wood in the longitudinal direction [12]. He concluded that a strain of 24% or more was necessary to produce crack initiation and considerable irreversible changes in the wood structure. Although this method has proven useful to detect the onset of cracking in samples, using it as a tool to quantify fatigue damage would require considerable further work.

Although not directly aimed at quantifying fibre separation, other work on the effect of cyclic loading has provided some insight into the energy dissipation processes associated with fatigue loading. From an analysis of video images captured during cyclic compression of loblolly pine, Hickey *et al*. [13] showed that the majority of the applied strain was supported by the earlywood regions. This was confirmed by Rudie *et al*. through temperature measurements [14]. They concluded that the majority of the energy input during cycling was dissipated in the earlywood.

In summary, although several methods have been used to monitor different aspects of damage accumulation under fatigue loading, none provides a direct measure of the extent of fibre separation. The present study delineates a direct approach to quantify the degree of fibre separation in samples subjected to fatigue loading. The proportion of separated fibres is measured by image analysis from micrographs obtained under a scanning electron microscope (SEM). A few simple processing steps are required which can be done using software available at no cost on the Internet. The image acquisition, image processing, and the calculation procedure are described here. The method was used to assess the effect of strain, strain rate, temperature, and number of cycles on samples subjected to repeated radial compression by processing micrographs obtained in previous studies [10,11].

SAMPLE PREPARATION AND LOADING

All tests were performed on samples 20mm X 20mm X 5mm in size in an MTS-858 servo-hydraulic machine. The test system and the instrumentation were described in Reference 9. All samples were subjected to repeated radial compression under displacement-controlled cycling. To study the effects of temperature, strain and strain rate, tests were conducted at two temperatures (25^{o}C and 96^{o}C), three levels of strain (30%, 50% and 70%), and two strain rates

($2.94s^{-1}$ and $20.8s^{-1}$). For the tests at 25°C, the samples were immersed in a water bath, while those at 96°C were kept in a steaming chamber. The latter was described in Reference 11. The sample preparation steps and the testing procedure were the same in all cases, and they have been described in Reference 10.

IMAGE ANALYSIS METHOD

Image processing

Images of samples at various stages of breakdown were acquired using a Hitachi scanning electron microscope. For each sample tested, gray scale images covering the entire transverse section were acquired at a resolution of 640 X 480 pixels (5.21 μ per pixel). At the magnification chosen, twelve images were required to cover the entire sample. The features of interest in these images in the context of mechanical pulping include cracks (their length, perimeter and path of propagation), changes in fibre diameter, the extent of fibrillation, and fibre wall deformations. This study focuses on fibre separation, and in particular on the quantification of the fibre separation index. Some simple processing steps are necessary on the acquired images to calculate this parameter. The images were processed and analysed on a Pentium™ 90 MHz computer using the free UTHSCSA ImageTool program. This program was developed at the University of Texas Health Science Center at San Antonio, Texas, and is available from the Internet by anonymous FTP at ftp://maxrad6.uthscsa.edu.

Image processing in this study involved the application of a median *filter*, an open operation and a *manual thresholding* step. A typical image acquired using the SEM is shown in **Figure 1a**. The *median filter* operation performs a low-pass filtering of the image by replacing each pixel in the image by the median value of the pixels immediately surrounding it. This removes non-uniform illumination, smooths the gray levels of the image histogram, and facilitates the *manual thresholding* operation performed at a later stage of image processing.

The *open* operation applies a sequence of three erosions followed by an equal number of dilations. Erosion operates by making white all black pixels that have a predetermined number of white neighbours. Dilation operates by making black any white pixels that have a predetermined number of black neighbours. The neighbourhood size in these operations is selected by the user and has to lie in the range of 1 to 8 pixels. A value of 8 pixels was used throughout this work. Lower values tend to have a more severe effect. The *open* operation produces a sharper image without noticeably changing the size or shape of individual objects or features. The gray scale image after these processing steps is shown in **Figure 1b**.

The next image processing step, *manual thresholding*, converts the gray scale image into a binary (black and white) image. This step is typically used in preparation for object identification. On activating the *manual thresholding* command in ImageTool, the user is presented with a histogram of the distribution of pixel values in the image and a double slider. Each value along the X-axis represents a gray level. The values along the Y-axis represent the number of pixels with that gray value in the image. As the sliders are moved, pixels with gray levels that fall between the two endpoints are arbitrarily set to black while pixels outside the range are set to white. The black and white image obtained by *manual thresholding* is shown in **Figure 1c**. Selection of the proper threshold was done by trial and error and was guided by visual inspection of the resulting binary image.

In summary, the image processing steps outlined above convert the acquired grey scale image (Figure 1a) into a binary image (Figure 1c) where points representing the fibre wall material appear in white, and fibre lumens and any area opened by fibre separation appear in black.

Crack identification and measurements

The next step involves identifying regions in the image where fibre separation has occurred. The *find objects* command in ImageTool was used for this purpose. This command identifies, in a binary image, objects defined by a minimum number of black pixels connected together. The minimum number of pixels is user-defined, and we used a value of eight in our analyses so that only cracks, and not fibre lumens, would be identified as objects. **Figure 1d** shows cracks that were identified as objects by the *find objects* command.

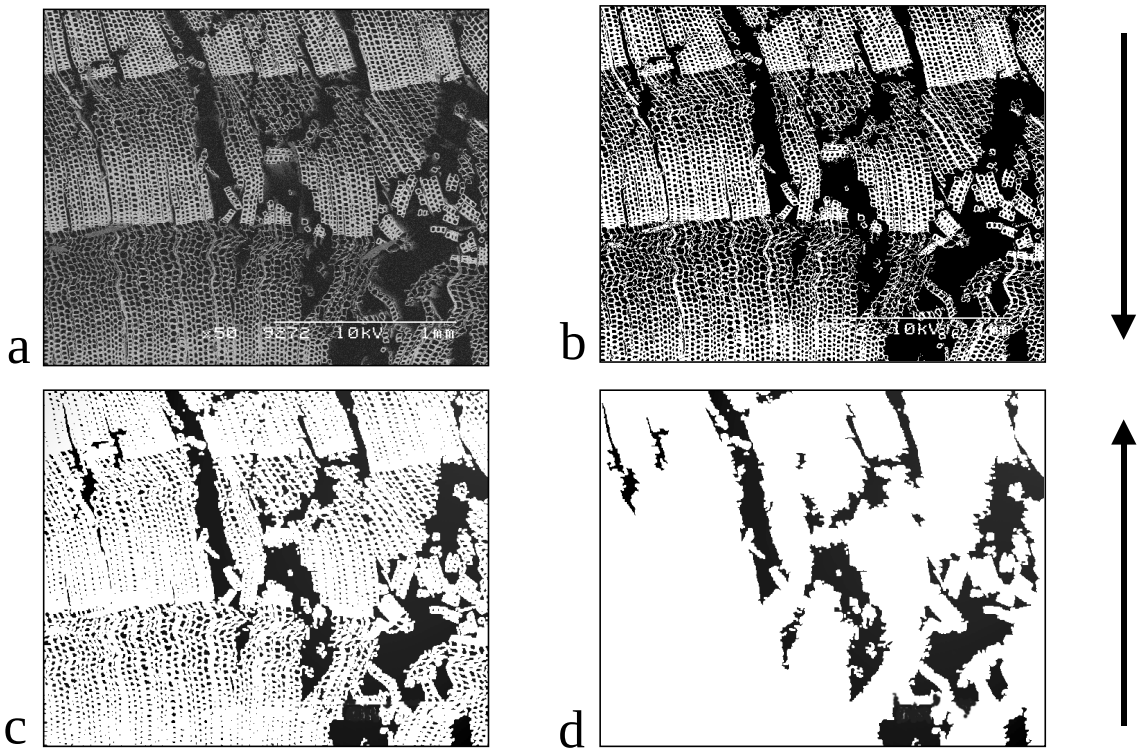

Figure 1. Typical micrographs illustrating the image processing steps required to isolate the cracks in a sample.

ImageTool has built-in functions to perform standard measurements on objects that have been identified and selected in the processed image. These were used to measure the size of all cracks in our images. However, absolute crack dimensions would appear to be a poor indicator of the degree of fibre separation, since fibre dimensions can vary between growth rings, trees and species. Instead, the fibre separation index in each sample was determined by calculating the ratio of the number of separated fibres and the total number of fibres in a sample. Evaluating the number of separated fibres requires proper care, since most fibres in the samples processed are not fully but only partially separated from the wood matrix. An accurate index of fibre separation has to account for these differences in the degree of separation when dealing with partly separated fibres. A relatively simple way of achieving this goal is to measure the projected

length of fibre surfaces exposed by cracks, and divide this total length by the average perimeter of a single fibre. This yields what can be thought of as an equivalent number of separated fibres.

Assuming that fibres have a square cross-section, each side having a length a, the equivalent number of separated fibres was obtained by taking the ratio of the total perimeter of the cracks in a sample, P_c, and the average perimeter of a fibre, $4a$.

$$\text{Equivalent number of separated fibres} = \frac{P_c}{4a} \tag{1}$$

The value of P_c was obtained using the built-in *perimeter* function in ImageTool. A spatial calibration was performed first, using the scale bar in a scanning electron micrograph, so that the perimeter measurement would reflect a quantity in millimeters. Since the imaged area was smaller than the sample cross-sectional area at the magnification chosen, a total of twelve images were required to cover the entire sample. The total perimeter of cracks in a sample was calculated by summing up the results from all twelve images collected for that sample.

The fibre width, a, was obtained by counting the number of fibres along lines of known length in each image, and averaging the results from all twelve images acquired for each sample. This was done before subjecting the samples to any loading. Since our images were rectangular in shape, we determined the number of fibres along lines (N_{x_i} and N_{y_i}) of length L_x and L_y drawn in the x and y-directions on the image of an untested sample. These measurements were facilitated by the *line profile* command in ImageTool. When applied to a line drawn on an image, the command displays a two-dimensional graph showing the intensities of pixels along the line. On a binary image, the number of peaks in the graph is a direct measure of the number of fibres along that line. Using N_{x_i}, N_{y_i}, L_x and L_y, the fibre width a_i in each image was calculated as:

$$a_i = \frac{1}{2}\left(\frac{L_x}{N_{x_i}} + \frac{L_y}{N_{y_i}}\right) \tag{2}$$

The final value of a for each sample was obtained by averaging the values of a_i corresponding to each of the twelve images acquired from that sample. Finally, the fibre separation index in a sample can be evaluated by dividing the equivalent number of separated fibres, as obtained from Eq. 1, by the total number of fibres in the sample:

$$\text{Fibre separation index} = \frac{P_c}{4a\sum_{i=1}^{12} N_{x_i} N_{y_i}} \tag{3}$$

RESULTS AND DISCUSSION

To evaluate the effect of strain, strain rate and temperature on the efficiency of fibre separation, fibre separation index was plotted against cumulative specific energy absorbed after 10, 25 and 100 cycles. The cumulative specific energy was calculated from the force and displacement data gathered during loading and the mass of each sample.

Figures 2 and **3** depict the fibre separation index as a function of cumulative specific energy absorbed (MJ/kg) at 25°C and 96°C, respectively. Each data point in these graphs represents the arithmetic average of six samples tested for each condition of strain, strain rate and temperature. The standard deviation of fibre separation index of these six samples is plotted as error bars for all conditions. Each line in the plots represents a specific combination of strain and strain rate, and the three points on a line correspond to values after 10, 25 and 100 cycles. Note that these lines were obtained from experiments performed under interrupted loading conditions, as outlined in References 10 and 11. The plots also show data points obtained after 100 cycles of uninterrupted loading. These points fall within acceptable range of the corresponding numbers for interrupted loading. This supports the idea that loading interruptions, which are necessary to observe the damage in samples at intermediate stages of cyclic loading, have little effect on the results.

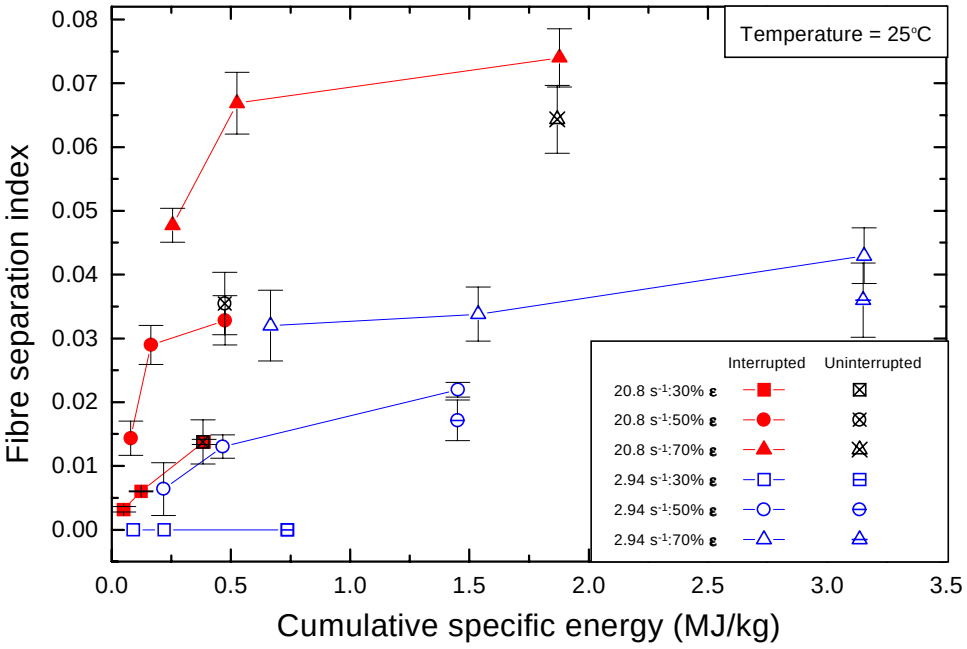

Figure 2. Fibre separation index vs. cumulative specific energy for cyclic loading at 25°C. Note that the first data point on the curves correspond to energy levels between 0.05 and 0.67 MJ/kg.

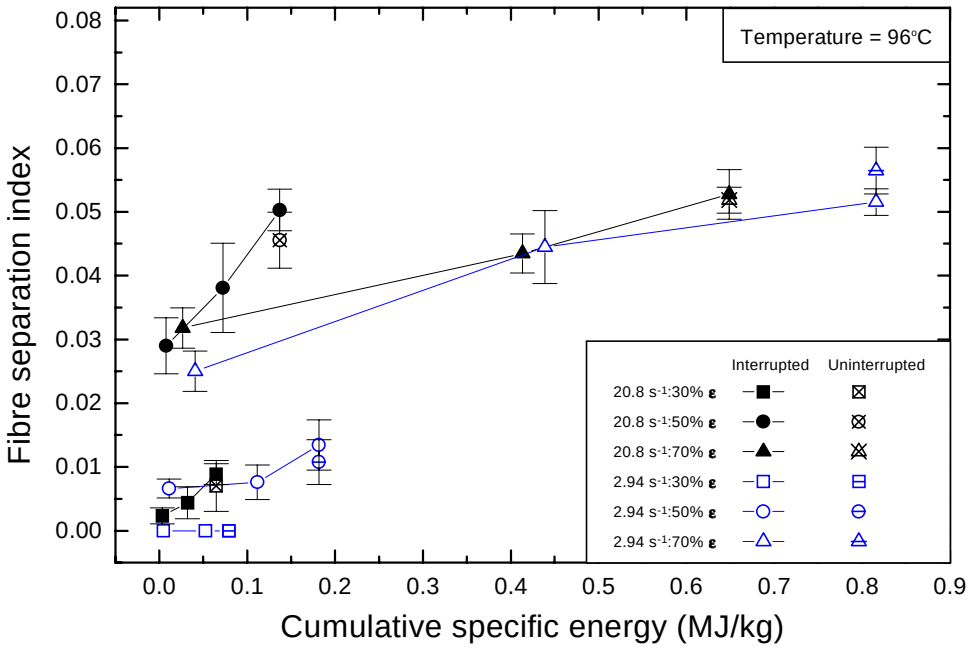

Figure 3. Fibre separation index vs. cumulative specific energy for cyclic loading at 96°C. Note that the first data point on the curves correspond to energy levels between 0.003 and 0.04 MJ/kg.

The results in Figures 2 and 3 confirm our earlier qualitative observations on the effect of strain, strain rate, temperature, and number of cycles [10,11]. Further, the quantitative nature of the results presented here also allows one to assess the efficiency of fibre separation in each case.

The results obtained at 25°C generally show a rapid initial increase in the fibre separation index, followed by a phase of comparatively less efficient fibre separation. We also know from earlier observations that the majority of cracks in the samples appear in the early stages of cycling [10], and further cycling tends to promote crack growth rather than crack initiation. This indicates that there is a marked difference in the efficiency with which the processes of crack initiation and propagation produce fibre separation. Finally, from these results, the most efficient loading condition for fibre separation corresponds to the highest strain and strain rate tested.

At 96°C, the results in Figure 3 indicate that the fibre separation index at a given combination of strain and strain rate is in most cases lower than at 25°C, but the energy required to achieve a given degree of fibre separation is much lower. The efficiency of fibre separation is thus comparatively much higher at this elevated temperature. Contrary to what we observed at the lower temperature, the efficiency of fibre separation remained relatively high with increased cycling.

SUMMARY AND CONCLUSIONS

A simple image analysis method has been developed to quantify fibre separation in wood samples subjected to fatigue loading. The fibre separation index, a parameter derived by processing and analyzing SEM images, was used to quantify the effect of strain, strain rate, and temperature. For each combination of loading conditions, the fibre separation index was

measured after 10, 25 and 100 cycles by interrupting the cyclic loading. Other results obtained after 100 cycles under uninterrupted cycling conditions showed that load interruptions have little effect on the results.

At 25°C, the results indicate that for a given specific energy expenditure, increasing strain or strain rate leads to a larger fibre separation index. For given loading conditions, the efficiency of fibre separation was generally seen to drop as cycling progressed. This was associated with a transition from a phase of crack initiation to one in which cracks already formed tended to propagate, which suggests that the process of crack initiation is more efficient for fibre separation. In general, the efficiency of fibre separation at 96°C was higher than at 25°C, and the efficiency of fibre separation did not decrease with increased cycling.

The results presented in this work refer to the effects of repeated compression on wood. The work is part of a larger project aimed at understanding the fundamental effects of compression and shear loading on chips in the early stage of breakdown by mechanical pulping. The results presented here cannot be used to draw conclusions on optimal primary refining conditions since the cycling frequency used in our study is many orders of magnitude smaller than that used in refining. It may be possible to extrapolate our results to a higher frequency with an approach similar to the one used by Salmén [15] to predict the viscoelastic properties of wood at high frequencies from measurements made at lower frequencies. Further work is required to verify if this approach is applicable to the fibre separation index evaluated in our study.

The image analysis method presented in this paper appears to be a reliable tool for the evaluation of fibre separation in wood due to fatigue damage. Although the method was applied only to samples loaded in radial compression, it is also applicable for samples loaded under any combination of shear and compressive loads. The authors know of no other method that would allow a direct comparison between these modes of loading.

REFERENCES

1. George E. R. Lamb. The efficiency of mechanical pulping processes. *Tappi Journal*, 43(11):939-944, 1960.
2. George E. R. Lamb. Energy consumption in mechanical pulping. *Pulp and Paper Magazine of Canada*, 63(3):T188-T191, T197, 1962.
3. D. Atack and W.D. May. Mechanical reduction of chips by double-disc refining. *Pulp and Paper Magazine of Canada*, 64:T75-T83, T118, 1963.
4. D. Atack, M.I. Stationwala, and A. Karnis. What happens in refining. *Pulp and Paper Canada*, 85(12):T303-308, 1984.
5. A. Karnis, D. Atack, and M.I. Stationwala. What happens in refining : 2. *Pulp and Paper Canada*, 87(11):T416-423, 1986.
6. L. Salmén and C. Fellers. The fundamentals of energy consumption during viscoelastic and plastic deformation of wood. *Transactions of the Technical Section*, CPPA, 8(4):TR93-99, 1982.
7. L. Salmén, A. Tigerström, and C. Fellers. Fatigue of wood – Characterization of mechanical defibration. *J. Pulp Paper Sci*., 11(3): J68-J73, 1985.
8. A. Uhmeier. *Some aspects on solid and fluid mechanics of wood in relation to mechanical pulping*. PhD thesis, Royal Institute of Technology, Stockholm, Div. Of Paper Technology, 1995.

9. R. Thiruvengadaswamy and D. Ouellet. On the generation of structural damage in wood by cyclic compressive loading. *J. Pulp Paper Sci*., 24(8): 247-253, 1998.
10. R. Thiruvengadaswamy and D. Ouellet. Structural breakdown in wood under cyclic compression at 25^{o}C. Pulp and Paper Research Institute of Canada, Post-Graduate Research Laboratory Report 712, October 1998. Submitted to Wood Science and Technology.
11. R. Thiruvengadaswamy and D. Ouellet. Structural breakdown in wood under cyclic compression at 96^{o}C. Pulp and Paper Research Institute of Canada, Post-Graduate Research Laboratory Report 741, November 1999. Submitted to Wood Science and Technology.
12. J. Berg. *Fracture behaviour of wood and fibre as related to the mechanical pulping processes*. Licentiate Thesis, Royal Institute of Technology, Stockholm, Dept. Of Pulp and Paper Chemistry and Technology, Div. Of Paper Technology, 1996.
13. K. L. Hickey and A. W. Rudie. Preferential energy absorption by earlywood in cyclic compression of Loblolly Pine. In *Eighteenth International Mechanical Pulping Conference, Oslo*, pages 81-86, 1993.
14. A. W. Rudie, J. Morra, J.M. St-Laurent, and K. L. Hickey. The influence of wood and fibre properties on mechanical pulping. *Tappi Journal*, 77(6): 86-90, 1994.
15. L. Salmén, "The effect of the frequency of a mechanical deformation on the fatigue of wood", *J. Pulp Paper Sci.*, 13(1):J23-J28, 1987.

Received: June 29, 1999
Revised: June 6, 2000
Accepted: July 3, 2000

This paper was accepted for abstracting and publication in the December 2000 issue of *TAPPI JOURNAL*.

TAPPI Website: www.tappi.org